paraffin-embedded (FFPE) tissue, BB cytology, and pleural effusion cytology samples from patients with NSCLC.

materials and methods

This was an observational study using control DNA admixtures and clinical samples. Patients provided written informed consent for samples to be used in research. The study was conducted as a collaborative research of AstraZeneca KK with National Cancer Center Hospital East (NCCHE) and Hyogo Cancer Center (HCC) after protocol approval by each Institutional Review Board and was conducted in accordance with ethical guidelines for epidemiological studies.

samples and DNA extraction

DNA admixtures

Four types of mutant plasmids were prepared including the *EGFR* mutation L858R, T790M, G719S, and E746-A750 deletion (nt del 2234-2249) in the Blue Heron pUC plasmid by Invitrogen Inc. (Tokyo, Japan). The sequence inserted into each plasmid corresponded with the longest sequence requirements spanning the exons across all of the methods to be evaluated, from −300 to +220 bp for exon 18 (for G719S) and from −200 to +200 bp for exons 19, 20, and 21 (for E746-A750 deletion, T790M, and L858R, respectively). Admixtures were prepared at Saitama Medical University Hospital. The plasmid preparations (5.4 ng/μl) were diluted with water and whole-human genomic DNA (12.5 ng/μl) (Promega Inc., Madison, WI) to prepare an admixture containing a 1 : 1 ratio (confirmed by Sanger sequencing) of copies of mutated and wild-type *EGFR* (5.4 fg/μl plasmid DNA, 10 ng/μl genomic DNA; referred to here as a 100% admixture). The 100% admixture solution was then diluted with genomic DNA to provide DNA solutions simulating those isolated from a clinical sample containing *EGFR*-mutated and wild-type cells at ratios of 50 : 50 (50% admixture), 25 : 75 (25%), 10 : 90 (10%), 5 : 95 (5%), 2 : 98 (2%), and 1 : 99 (1%). The samples were divided into aliquots for each laboratory, randomized and assigned an identification code, and 20 μl of each sample sent to the laboratories for mutation testing in a blinded manner. Ten wild-type control samples (from a single stock of genomic DNA) (10 ng/μl) were also distributed for testing.

formalin-fixed paraffin-embedded samples

In total, 120 FFPE NSCLC samples collected at NCCHE ($n = 100$) and HCC ($n = 20$) between December 2005 and October 2009 were used. Twelve consecutive sections (5-μm thickness), prepared by Sanritsu Co. Ltd (Tokyo, Japan) from each FFPE tissue block, were allocated as follows: sections 1 and 12, hematoxylin–eosin (H&E) staining; sections 2 and 7, PCR direct sequencing; sections 3 and 8, Cycleave PCR; sections 4 and 9, PCR-Invader; sections 5 and 10, PNA-LNA PCR clamp; sections 6 and 11, Scorpion ARMS. Samples were randomly assigned an identification code by Sanritsu Co. Ltd, with separate identification codes for the samples for PCR direct sequencing and Cycleave PCR (as they were to be analyzed by the same laboratory). A table of corresponding randomized identification codes was retained by AstraZeneca KK until analysis. H&E-stained sections (Sanritsu Co. Ltd) were reviewed by a single pathologist at NCCHE for histological type, tumor cell content, and tumor dimension in a blinded manner. DNA was extracted at each testing laboratory using their own standard operating procedures (SOPs), all of which utilized the QIAamp kit (QIAGEN Japan, Tokyo, Japan) (see supplemental Methods, available at *Annals of Oncology* online).

bronchofiberscopic brushing cytology samples

Thirty BB cytology samples (with matched FFPE samples available) obtained at NCCHE ($n = 10$) and HCC ($n = 20$) between 2006 and 2009 were used. Samples were collected by exfoliative cytodiagnosis brushing or curette washing in saline solution, without anticoagulant, and stored frozen. The BB cytology samples were randomized and assigned an identification code. The presence of tumor cells and histological type were confirmed by a pathologist at each center. DNA was extracted (QIAamp DNA Mini kit, QIAGEN Japan) at Kinki University of Medicine (Department of Genome Biology) and divided into 22 μl aliquots for analysis by the testing laboratories (direct sequencing was excluded due to the small amount of DNA anticipated, and for Scorpion ARMS, if the DNA concentration was <1 ng/μl, only exon 19 deletions, L858R, and T790M mutations were analyzed—see supplemental Methods, available at *Annals of Oncology* online).

pleural effusion cytology samples

Pleural effusion cytology samples were provided by NCCHE. Twenty pleural effusion cytology samples were collected from patients diagnosed with NSCLC (adenocarcinoma) between February 2009 and February 2010 and confirmed by a pathologist to contain tumor cells. Samples were frozen within 10 and 30 min of sampling and stored at −80°C. Frozen samples were thawed at 37°C and refrozen rapidly three times to disrupt the cells and ensure an even distribution and then divided into five equal aliquots that were sent to each of the testing laboratories. Samples were randomly assigned an identification code as for the FFPE samples. DNA was extracted at each laboratory using their own SOPs, all of which were based on the use of the QIAamp kit (see supplemental Methods, available at *Annals of Oncology* online).

EGFR mutation analysis

Samples were analyzed using five different *EGFR* mutation tests carried out by four different testing laboratories: PCR-Invader [4, 12] by BML Inc. (Tokyo, Japan); PNA-LNA PCR clamp [5] by Mitsubishi Chemical Medience Corp. (Tokyo, Japan); PCR direct sequencing (with the exception of the BB cytology samples, due to the anticipated tumor DNA yield based on published evidence regarding the detection limit of this method [13]) [6] by SRL Inc. (Tokyo, Japan), Cycleave PCR [7] also by SRL Inc., and Scorpion ARMS [14, 15] by Genzyme Analytical Services (Los Angeles, CA). Scorpion ARMS analysis employed the DxS *EGFR* Mutation Test Kit for research use only [QIAGEN Manchester (formerly DxS Ltd), UK] and was carried out according to the manufacturer's instructions with modifications described in the supplemental Methods (available at *Annals of Oncology* online). The other methods were carried out using each of the laboratories' experimental set up, with data analysis and quality control completed according to their own specific protocols (further details in the supplemental Methods, available at *Annals of Oncology* online). Samples were defined as mutation negative where sufficient material was present to generate a result but the presence of a mutation was not observed within the detection limit of the assay. The *EGFR* mutations detected by each *EGFR* mutation test are shown in supplemental Table S1 (available at *Annals of Oncology* online).

Analysis data (positive, negative, not detected, mutation type) and any supplemental information (e.g. failure of PCR amplification) were reported to AstraZeneca KK (Osaka, Japan).

statistical analysis

The correct determination rates (whether or not the positive/negative *EGFR* mutation assessment result was correct) and sensitivity (lowest percentage DNA admixture detected) by *EGFR* mutation type were assessed using DNA admixture samples for each *EGFR* mutation test.

The success and positive rates of each *EGFR* mutation test were determined using FFPE, and BB and pleural effusion cytology samples. The success rate was defined as the proportion of samples successfully analyzed

where it was possible to determine the mutation status. Samples were classified as unsuccessful where it was not possible to determine the mutation status, the PCR amplification failed, or if values of samples exceeded the cut-off value of Scorpion ARMS. The positive rate was defined as the number of samples analyzed as positive by each method as a proportion of the number of samples successfully analyzed. False-positive and false-negative rates were not determined, as no reference or 'gold standard' has been defined for *EGFR* mutation analysis.

The concordance rates and Cohen's kappa coefficients were determined between different methods of detection and between FFPE versus BB cytology sample types for mutation types commonly detectable by all assessed methods. Cohen's kappa coefficient was calculated as: kappa = (Po–Pe)/(1–Pe), where Po is the observed concordance rate and Pe is the expected probability of chance agreement.

results

patient samples

In total, 116 FFPE samples were evaluable for analysis, as four samples were confirmed not to contain NSCLC cells. The majority of samples were of adenocarcinoma histology and had a tumor cell content of at least 50%. Both tissue and tumor dimensions were ≤19 mm in most samples.

Of the 30 BB cytology samples (24 adenocarcinoma, four squamous, one adenosquamous, one large cell), one sample was excluded from the analysis because its matching FFPE sample was not judged as NSCLC. The samples were taken at a mean of 39 days (range 20–70 days) before operation and the mean DNA concentration was 8.73 ng/μl (range 0.2–40.3 ng/μl). All 20 pleural effusion cytology samples were assessable for analysis. Volumes of pleural effusion cytology samples used for each test method were 0.7–0.8 ml.

comparability of five *EGFR* mutation tests

DNA admixtures

PCR-Invader, PNA-LNA PCR clamp, Cycleave PCR, and Scorpion ARMS methods detected each of the *EGFR* mutation types L858R, T790M, G719S, and the in-frame deletion E746-A750 type I at ratios ranging from 1% to 50% of mutant/wild-type allele. PCR direct sequencing detected all types of mutations in samples containing 5%–50% of plasmid DNA but could not detect any of the mutations in the 1% mutant DNA admixture, nor exon 19 deletion or L858R in the 2% mutant DNA admixture. There were no false positives in wild-type samples.

formalin-fixed paraffin-embedded samples

Success rates of all five *EGFR* mutation tests were over 90% in FFPE samples (Table 1). Concordance rates between any two methods ranged from 85.3% to 99.1% including samples unsuccessfully analyzed and from 94.3% to 100% excluding samples unsuccessfully analyzed (supplemental Table S2, available at *Annals of Oncology* online). The rate of type 1 discordance (different mutations detected between the methods) was 3.4% (4/116 samples) and the rate of type 2 discordance (mismatch of mutation status between the methods) was 6.9% (8/116 samples) in FFPE samples (supplemental Table S3, available at *Annals of Oncology* online).

Unsuccessful rates of mutation analyses and discordance rates by tumor/sample characteristics for FFPE samples are shown in supplemental Figure S1 (available at *Annals of Oncology* online). Higher unsuccessful rates were associated with histological subtype [squamous cell carcinoma, 4/7 (57.1%)], older sample age [year of surgery 2006, 9/10 (90.0%)], and larger tumor dimension [20–29 mm, 3/15

Table 1. Success rate and *EGFR* mutation status determined by different *EGFR* mutation tests in FFPE, BB, and pleural effusion samples

Sample type and method	No. of samples successfully analyzed (%)	No. of mutation-positive samples (%)[a]	No. of mutation-negative samples (%)[a]
FFPE samples ($n = 116$)			
Scorpion ARMS	115 (99.1)	65 (56.5)	50 (43.5)
PCR-Invader	116 (100.0)	65 (56.0)	51 (44.0)
PNA-LNA PCR clamp	106 (91.4)	61 (57.5)	45 (42.5)
PCR direct sequencing	110 (94.8)	64 (58.2)	46 (41.8)
Cycleave PCR	116 (100.0)	63 (54.3)	53 (45.7)
BB cytology samples ($n = 29$)			
Scorpion ARMS	29 (100.0)	15 (51.7)	14 (48.3)
PCR-Invader	29 (100.0)	17 (58.6)	12 (41.4)
PNA-LNA PCR clamp	29 (100.0)	17 (58.6)	12 (41.4)
Cycleave PCR	29 (100.0)	16 (55.2)	13 (44.8)
Pleural effusion cytology samples ($n = 20$)			
Scorpion ARMS	20 (100.0)	11 (55.0)	9 (45.0)
PCR-Invader	20 (100.0)	11 (55.0)	9 (45.0)
PNA-LNA PCR clamp	20 (100.0)	10 (50.0)	10 (50.0)
PCR direct sequencing	20 (100.0)	11 (55.0)	9 (45.0)
Cycleave PCR	20 (100.0)	11 (55.0)	9 (45.0)

[a]Percentage calculated based on the number of samples successfully analyzed; *EGFR* mutation status was determined before the study and samples were selected to allow for an ~1 : 1 ratio of mutation-positive : mutation-negative samples.

ARMS, Amplification Refractory Mutation System; BB, bronchofiberscopic brushing; FFPE, formalin-fixed paraffin-embedded; PNA-LNA, peptide nucleic acid-locked nucleic acid.

(20.0%)] (supplemental Figure S1, available at *Annals of Oncology* online). Discordance rates tended to be higher in samples with low tumor cell content [0–20%, 2/10 (20.0%); 30–40%, 3/10 (30%)], smaller tumor dimension [0–9 mm, 11/53 (20.8%)], smaller tissue dimension [0–9 mm, 8/33 (24.2%)], and older sample age [year of surgery 2006, 2/10 (20.0%)] (supplemental Figure S1, available at *Annals of Oncology* online).

Concordance rates between five methods for the two major mutation types in FFPE samples were 81.8% (18/22) for exon 19 deletions and 87.2% (34/39) for L858R.

PCR direct sequencing identified rare mutations in six patients that were not detected by any other methods [V689L and E690V, E709V, V834L, I706T D770_N771 (insSVD), H773_V774(insPH)].

bronchofiberscopic brushing cytology samples

Success rates of the four *EGFR* mutation tests utilized for analysis of BB cytology samples were 100% (Table 1) and concordance rates between two methods ranged from 93.1% to 100% (supplemental Table S2, available at *Annals of Oncology* online). Discordances between two methods were found in two (6.9%) samples (supplemental Table S4, available at *Annals of Oncology* online). Both were type 2 discordances (mismatch of mutation status between the methods): in one sample, G719C detected by PCR-Invader and PNA-LNA PCR clamp was assessed as negative by Cycleave PCR (G719X not analyzed by Scorpion ARMS due to insufficient sample). In the remaining sample, L858R detected by PCR-Invader, PNA-LNA PCR clamp, and Cycleave PCR was assessed as negative by Scorpion ARMS.

Concordance rates between analysis of BB cytology and FFPE samples ranged from 65.5% to 96.6% including samples unsuccessfully analyzed and 93.1%–96.6% excluding samples unsuccessfully analyzed (supplemental Table S5, available at *Annals of Oncology* online). Discordances in analysis of BB cytology samples versus FFPE samples by the same detection method (excluding discordances due to unsuccessful mutation analysis of FFPE samples) were observed in three (10.3%) samples (supplemental Table S4, available at *Annals of Oncology* online); all were type 2 discordances (mismatch of mutation status between the methods).

pleural effusion cytology samples

Success rates of all five *EGFR* mutation tests were 100% (Table 1) and concordance rates between two methods ranged from 85.0% to 100% in the pleural effusion samples (supplemental Table S2, available at *Annals of Oncology* online). Discordances between five methods were found in three (15.0%) samples (supplemental Table S6, available at *Annals of Oncology* online). All were type 2 discordances (mismatch of mutation status between the methods): in one sample, an exon 19 deletion was detected by all methods except PCR direct sequencing; in another, an exon 19 deletion was only detected by Scorpion ARMS, Cycleave PCR, and PCR direct sequencing; and in the third sample, L858R was only detected by PCR-Invader. In one of the other 17 samples, PCR direct sequencing detected an additional mutation [exon 18 deletion (E709_T710>D)], which the other methods were not designed to assess.

discussion

Analysis of the control DNA admixture samples showed that the *EGFR* mutation tests had comparable sensitivity, with the exception of direct sequencing. The sensitivity of direct sequencing, although higher than expected and reported elsewhere [15], was lower than the other techniques.

The results of this study showed that all five *EGFR* mutation tests had comparable success rates (over 90%) in FFPE samples. These were consistently high success rates given that the fixation of some of the samples was not ideal (e.g. long fixation times). The success rates of direct sequencing were higher than anticipated based on previous studies of clinical samples. For example, in a recent study, ARMS and direct sequencing were used to detect known *EGFR* mutations in NSCLC FFPE samples, and ARMS was found to be a more sensitive and robust technique [13]. However, it should be recognized that even when utilizing the same technologies, differences in reagents, DNA quality, software, and crucially, primer design and amplicon size have a huge influence on direct sequencing success rates and mutation detection potential. Our results show that the processes implemented by the laboratory in this study are highly optimized for the detection of *EGFR* mutations from tumor DNA using direct sequencing. As the testing laboratories also carried out the DNA extraction (with the exception of BB cytology samples), the slight differences in DNA extraction and processes across the different laboratories could also impact on the overall performance of the test methods.

All the FFPE samples were examined by a pathologist and generally found to be of high quality and tumor content. The numbers of samples with different tumor/sample characteristics were too low to make any definitive conclusions regarding unsuccessful and discordance rates by these characteristics. However, sample unsuccessful rates appear to be associated with squamous cell carcinoma, older samples, and samples with long tumor dimension, all of which can make it difficult to extract DNA. In addition, discordance rates appeared higher in older samples or samples of low tumor cell content, short tumor dimension or short tissue dimension, where the quantities of DNA are small.

Concordance rates were generally over 85% (>94%, excluding samples unsuccessfully analyzed) between any two *EGFR* mutation tests in FFPE samples. The lowest concordance rates between the five methods were in comparison with the PNA-LNA PCR clamp method. As the PNA-LNA PCR clamp method also had a higher unsuccessful rate than the other methods, concordance rates were lower in comparison with other methods when including samples unsuccessfully analyzed. However, all kappa statistics were ≥ 0.70, indicating a high concordance of analysis results. Concordance rates for the two major *EGFR* mutation types, exon 19 deletions and L858R, across the five mutation tests in FFPE samples were also high (81.8% and 87.2%, respectively), illustrating the suitability of all

five methods for *EGFR* mutation analysis in clinical studies and diagnostic applications. However, as the concordance rates were not 100% for any one method, we would advocate the selection of a single method for consistent use during a clinical study. With regard to daily practice, the decision to select and adopt a particular technology is at the discretion of individual laboratories and may be influenced by the diagnostic environment in which they reside. Selection factors may include technical expertise of operators, cost, test status (*in vitro* diagnostic versus laboratory-developed test), or availability of instrumentation.

Several factors may have contributed to the discordances between the *EGFR* mutation tests. These factors may have included differences in sensitivity and specificity, different DNA extraction procedures between laboratories, variation in tumor cell content within and across samples, and tumor heterogeneity within an FFPE block [10, 11, 16].

The performance of all five *EGFR* mutation tests was comparable in the analysis of both BB and pleural effusion cytology samples, with 100% success rates. BB cytology samples showed high concordance rates (>93%, excluding samples unsuccessfully analyzed) between pairs of *EGFR* mutation tests and versus FFPE samples by each detection method. Using the PNA-LNA PCR clamp method, analysis of BB cytology samples was successful where the matched FFPE sample failed analysis. Some mutations were detected in cytology samples of low DNA concentrations where matching FFPE samples were assessed as mutation negative. This result suggests that cytology samples can be useful in mutation analysis when tissue samples cannot be used, are in a small quantity, or degradation of FFPE samples is suspected. Pleural effusion cytology samples may be particularly suitable for analysis as they can be obtained easily, non-invasively and repeatedly, and generally contain plenty of cancer cells, relative to other sample types.

To our knowledge, this is the first high-quality comparison study of *EGFR* mutation tests in both FFPE and cytology samples. The results of the current study indicate that cytology-derived DNA is a suitable alternative to FFPE samples for the analysis of *EGFR* mutations and may be useful when FFPE samples are unavailable for molecular analysis. Other studies have also shown that ARMS can be used to detect *EGFR* mutations in cytology samples from transbronchial needle aspirates [17] or pleural effusion [18] and that this technique appeared to be more sensitive than direct sequencing in this sample type. Other methods for *EGFR* mutation testing, including pyrosequencing [19] and high-resolution melting analysis [20], also exist.

In summary, the performance of all five *EGFR* mutation tests was comparable in the analysis of FFPE and cytology samples. Where *EGFR* mutation tests and standard operating procedures are used in a reliable robust way, with trained operators, in a well-developed diagnostic setting, comparable results are obtained across mutation tests and sample types. FFPE specimens are currently the sample of choice for determining *EGFR* mutation status [11]. However, the ability to use cytology samples allows additional patients to be tested for *EGFR* mutations, and therefore, more appropriate treatment of their disease.

acknowledgements

We thank Annette Smith, PhD, from Complete Medical Communications, who provided medical writing support funded by AstraZeneca.

funding

This work was supported by AstraZeneca. AstraZeneca employees participated in the conception and design of the study, collection and assembly of data, data analysis, and interpretation.

disclosure

KG has received honoraria from Ono Pharmaceutical and Chugai Pharmaceutical and fees for consultancy/advisory boards from Ono Pharmaceutical. MS has received honoraria from Chugai Pharmaceutical and AstraZeneca. KN has received research grants from Daiichi Sankyo, Chugai Pharmaceutical, AstraZeneca, Glaxo SmithKline, and Solasia Pharma KK, research support from Chugai Pharmaceutical, and honoraria from Kyowa Hakko Kirin, Sumitomo Bakelite, Taiho Pharmaceutical, and Qiagen. KH has received patent fees from Mitsubishi Chemical Medience. TM has received honoraria from AstraZeneca and Chugai Pharmaceutical. JW, ED, RM, and TT are employees of AstraZeneca and hold stock in AstraZeneca. GI has declared no conflicts of interest.

references

1. Mok TS, Wu Y-L, Thongprasert S et al. Gefitinib or carboplatin-paclitaxel in pulmonary adenocarcinoma. N Engl J Med 2009; 361: 947–957.
2. Mitsudomi T, Morita S, Yatabe Y et al. Gefitinib versus cisplatin plus docetaxel in patients with non-small-cell lung cancer harbouring mutations of the epidermal growth factor receptor (WJTOG3405): an open label, randomised phase 3 trial. Lancet Oncol 2010; 11: 121–128.
3. Maemondo M, Inoue A, Kobayashi K et al. Gefitinib or chemotherapy for non-small-cell lung cancer with mutated EGFR. N Engl J Med 2010; 362: 2380–2388.
4. Hall JG, Eis PS, Law SM et al. Sensitive detection of DNA polymorphisms by the serial invasive signal amplification reaction. Proc Natl Acad Sci U S A 2000; 97: 8272–8277.
5. Nagai Y, Miyazawa H, Huqun et al. Genetic heterogeneity of the epidermal growth factor receptor in non-small cell lung cancer cell lines revealed by a rapid and sensitive detection system, the peptide nucleic acid-locked nucleic acid PCR clamp. Cancer Res 2005; 65: 7276–7282.
6. Lynch TJ, Bell DW, Sordella R et al. Activating mutations in the epidermal growth factor receptor underlying responsiveness of non-small-cell lung cancer to gefitinib. N Engl J Med 2004; 350: 2129–2139.
7. Yatabe Y, Hida T, Horio Y et al. A rapid, sensitive assay to detect EGFR mutation in small biopsy specimens from lung cancer. J Mol Diagn 2006; 8: 335–341.
8. Kimura H, Kasahara K, Kawaishi M et al. Detection of epidermal growth factor receptor mutations in serum as a predictor of the response to gefitinib in patients with non-small-cell lung cancer. Clin Cancer Res 2006; 12: 3915–3921.
9. Yamamoto N, Ichinose Y, Nishiwaki Y et al. EGFR mutations based on circulating free DNA in the subset of Japanese patients from IPASS (IRESSA Pan Asia Study), a phase III study of first-line gefitinib vs carboplatin/paclitaxel in clinically selected patients with advanced non-small-cell lung cancer. Poster 78 presented at EORTC-NCI-ASCO. Brussels, Belgium 2009; 15–17 October.
10. Eberhard DA, Giaccone G, Johnson BE. Biomarkers of response to epidermal growth factor receptor inhibitors in non-small-cell lung cancer working group:

standardization for use in the clinical trial setting. J Clin Oncol 2008; 26: 983–994.
11. Pirker R, Herth FJ, Kerr KM et al. Consensus for EGFR mutation testing in non-small cell lung cancer: results from a European workshop. J Thorac Oncol 2010; 5: 1706–1713.
12. Naoki K, Soejima K, Okamoto H et al. The PCR-invader method (structure-specific 5' nuclease-based method), a sensitive method for detecting EGFR gene mutations in lung cancer specimens; comparison with direct sequencing. Int J Clin Oncol 2011; 16: 335–344.
13. Ellison G, Donald E, McWalter G et al. A comparison of ARMS and DNA sequencing for mutation analysis in clinical biopsy samples. J Exp Clin Cancer Res 2010; 29: 132.
14. Newton CR, Graham A, Heptinstall LE et al. Analysis of any point mutation in DNA. The amplification refractory mutation system (ARMS). Nucleic Acids Res 1989; 17: 2503–2516.
15. Whitcombe D, Theaker J, Guy SP et al. Detection of PCR products using self-probing amplicons and fluorescence. Nat Biotechnol 1999; 17: 804–807.
16. Oliner K, Juan T, Suggs S et al. A comparability study of 5 commercial KRAS tests. Diagn Pathol 2010; 5: 23.
17. Horiike A, Kimura H, Nishio K et al. Detection of epidermal growth factor receptor mutation in transbronchial needle aspirates of non-small cell lung cancer. Chest 2007; 131: 1628–1634.
18. Kimura H, Fujiwara Y, Sone T et al. High sensitivity detection of *epidermal growth factor receptor* mutations in the pleural effusion of non-small cell lung cancer patients. Cancer Sci 2006; 97: 642–648.
19. Takano T, Ohe Y, Sakamoto H et al. Epidermal growth factor receptor gene mutations and increased copy numbers predict gefitinib sensitivity in patients with recurrent non-small-cell lung cancer. J Clin Oncol 2005; 23: 6829–6837.
20. Willmore-Payne C, Holden JA, Layfield LJ. Detection of epidermal growth factor receptor and human epidermal growth factor receptor 2 activating mutations in lung adenocarcinoma by high-resolution melting amplicon analysis: correlation with gene copy number, protein expression, and hormone receptor expression. Hum Pathol 2006; 37: 755–763.

Annals of Oncology 23: 2919–2924, 2012
doi:10.1093/annonc/mds123
Published online 10 July 2012

Prophylactic cranial irradiation in small-cell lung cancer: Findings from a North Central Cancer Treatment Group Pooled Analysis

S. E. Schild[1*], N. R. Foster[2], J. P. Meyers[2], H. J. Ross[3], P. J. Stella[4], Y. I. Garces[5], K. R. Olivier[5], J. R. Molina[6], L. R. Past[7] & A. A. Adjei[5] on behalf of North Central Cancer Treatment Group

[1]Department of Radiation Oncology, Mayo Clinic, Scottsdale; [2]Section of Biomedical Statistics and Informatics, Mayo Clinic, Rochester; [3]Division of Medical Oncology, Mayo Clinic; [4]Michigan Cancer Research Consortium, Ann Arbor; [5]Department of Radiation Oncology, Mayo Clinic, Rochester; [6]Department of Medical Oncology, Mayo Clinic, Rochester; [7]Department of Radiation Oncology, Luther Hospital Eau Claire; [8]Department of Medicine, Roswell Park Cancer Institute, Buffalo, USA

Received 20 January 2012; revised 12 March 2012; accepted 14 March 2012

Background: This pooled analysis evaluated the outcomes of prophylactic cranial irradiation (PCI) in 739 small-cell lung cancer (SCLC patients with stable disease (SD) or better following chemotherapy ± thoracic radiation therapy (TRT) to examine the potential advantage of PCI in a wider spectrum of patients than generally participate in PCI trials.
Patients and methods: Three hundred eighteen patients with extensive SCLC (ESCLC) and 421 patients with limited SCLC (LSCLC) participated in four phase II or III trials. Four hundred fifty-nine patients received PCI (30 Gy/15 or 25 Gy/10) and 280 did not. Survival and adverse events (AEs) were compared.
Results: PCI patients survived significantly longer than non-PCI patients {hazard ratio [HR] = 0.61 [95% confidence interval (CI): 0.52–0.72]; $P < 0.0001$}. The 1- and 3-year survival rates were 56% and 18% for PCI patients versus 32% and 5% for non-PCI patients. PCI was still significant after adjusting for age, performance status, gender, stage, complete response, and number of metastatic sites (HR = 0.82, $P = 0.04$). PCI patients had significantly more grade 3+ AEs (64%) compared with non-PCI patients (50%) ($P = 0.0004$). AEs associated with PCI included alopecia and lethargy. Dose fractionation could be compared only for LSCLC patients and 25 Gy/10 was associated with significantly better survival compared with 30 Gy/15 (HR = 0.67, $P = 0.018$).
Conclusions: PCI was associated with a significant survival benefit for both ESCLC and LSCLC patients who had SD or a better response to chemotherapy ± TRT. Dose fractionation appears important. PCI was associated with an increase in overall and specific grade 3+ AE rates.
Key words: PCI, prophylactic cranial irradiation, radiotherapy, small-cell lung cancer, survival

*Corresponding author: Dr S. E. Schild, Department of Radiation Oncology, Mayo Clinic, 5777 East Mayo Boulevard, Phoenix, AZ 85255, USA. Tel: +1-480-301-8133; Fax: +1-480-301-7687; E-mail: sschild@mayo.edu

Published OnlineFirst June 22, 2012; DOI: 10.1158/1535-7163.MCT-11-0934

Molecular Cancer Therapeutics

Antitumor Action of the MET Tyrosine Kinase Inhibitor Crizotinib (PF-02341066) in Gastric Cancer Positive for *MET* Amplification

Wataru Okamoto, Isamu Okamoto, Tokuzo Arao, et al.

Mol Cancer Ther 2012;11:1557-1564. Published OnlineFirst June 22, 2012.

Published OnlineFirst June 22, 2012; DOI: 10.1158/1535-7163.MCT-11-0934

Molecular Cancer Therapeutics

Preclinical Development

Antitumor Action of the MET Tyrosine Kinase Inhibitor Crizotinib (PF-02341066) in Gastric Cancer Positive for *MET* Amplification

Wataru Okamoto[1], Isamu Okamoto[1], Tokuzo Arao[2], Kiyoko Kuwata[1], Erina Hatashita[1], Haruka Yamaguchi[1], Kazuko Sakai[2], Kazuyoshi Yanagihara[3], Kazuto Nishio[2], and Kazuhiko Nakagawa[1]

Abstract

Therapeutic strategies that target the tyrosine kinase MET hold promise for gastric cancer, but the mechanism underlying the antitumor activity of such strategies remains unclear. We examined the antitumor action of the MET tyrosine kinase inhibitor crizotinib (PF-02341066) in gastric cancer cells positive or negative for *MET* amplification. Inhibition of MET signaling by crizotinib or RNA interference–mediated MET depletion resulted in induction of apoptosis accompanied by inhibition of AKT and extracellular signal–regulated kinase phosphorylation in gastric cancer cells with *MET* amplification but not in those without it, suggesting that MET signaling is essential for the survival of *MET* amplification–positive cells. Crizotinib upregulated the expression of BIM, a proapoptotic member of the Bcl-2 family, as well as downregulated that of survivin, X-linked inhibitor of apoptosis protein (XIAP), and c-IAP1, members of the inhibitor of apoptosis protein family, in cells with *MET* amplification. Forced depletion of BIM inhibited crizotinib-induced apoptosis, suggesting that upregulation of BIM contributes to the proapoptotic effect of crizotinib. Crizotinib also exhibited a marked antitumor effect in gastric cancer xenografts positive for *MET* amplification, whereas it had little effect on those negative for this genetic change. Crizotinib thus shows a marked antitumor action both *in vitro* and *in vivo* specifically in gastric cancer cells positive for *MET* amplification. *Mol Cancer Ther; 11(7); 1557–64. ©2012 AACR.*

Introduction

Gastric cancer is the second most frequent cause of cancer deaths worldwide (1). Chemotherapy has a beneficial effect on survival in individuals with advanced-stage gastric cancer, but even so overall survival is usually still only about 1 year (1, 2). Substantial advances in the development of molecularly targeted therapies for gastric cancer have been achieved in recent years (3). Amplification of the proto-oncogene *MET* is a frequent molecular abnormality in gastric cancer (4–6), and a MET-tyrosine kinase inhibitor (TKI) has been shown to induce apoptosis in gastric cancer cells with *MET* amplification (7, 8).

Crizotinib (PF-02341066; Fig. 1A) was recently approved by the U.S. Food and Drug Administration (FDA) for the treatment of patients with lung cancer positive for fusion of the echinoderm microtubule-associated protein–like 4 (*EML4*) and anaplastic lymphoma kinase (*ALK*) genes. This agent also inhibits MET in addition to oncogenic fusion variants of the tyrosine kinase ALK (9, 10), and it may thus be an attractive therapeutic option for individuals with gastric cancer positive for *MET* amplification. We have therefore now investigated the effects of crizotinib on cell survival and signal transduction in gastric cancer cells with *MET* amplification. We further examined the molecular mechanism underlying the antitumor action of MET inhibition.

Authors' Affiliations: Departments of [1]Medical Oncology and [2]Genome Biology, Kinki University Faculty of Medicine, Osaka-Sayama, Osaka; and [3]Laboratory of Health Sciences, Department of Life Sciences, Yasuda Women's University Faculty of Pharmacy, Asaminami, Hiroshima, Japan

Note: Supplementary data for this article are available at Molecular Cancer Therapeutics Online (http://mct.aacrjournals.org/).

Corresponding Author: Isamu Okamoto, Department of Medical Oncology, Kinki University Faculty of Medicine, 377-2 Ohno-higashi, Osaka-Sayama, Osaka 589-8511, Japan. Phone: 81-72-366-0221; Fax: 81-72-360-5000; E-mail: chi-okamoto@dotd.med.kindai.ac.jp

doi: 10.1158/1535-7163.MCT-11-0934

Materials and Methods

Cell culture and reagents

Human gastric cancer cell lines positive (SNU5, Hs746T, MKN45, HSC58, 58As1, 58As9) or negative (SNU1, N87, AGS, MKN1, MKN7, NUGC3, AZ521, MKN28, HSC39, SNU216) for *MET* amplification were obtained as previously described (8, 11). All cells were cultured under a humidified atmosphere of 5% CO_2 at 37°C in RPMI-1640 medium (Sigma) supplemented with 10% FBS and were passaged for ≤3 months before renewal from frozen early-passage stocks obtained from the respective sources. Cells were regularly screened for mycoplasma with the use of a MycoAlert Mycoplasma detection kit (Lonza). Crizotinib was kindly provided by

Published OnlineFirst June 22, 2012; DOI: 10.1158/1535-7163.MCT-11-0934

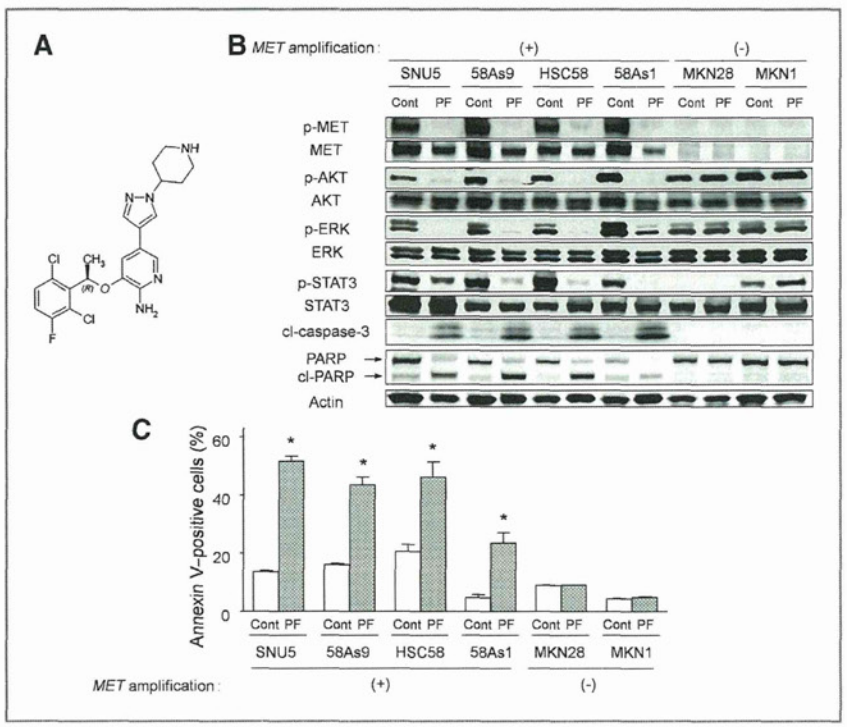

Figure 1. Effects of crizotinib on MET, AKT, ERK, and STAT3 phosphorylation, as well as on apoptosis in human gastric cancer cells. A, structure of crizotinib. B, the indicated cell lines were incubated in the absence (Cont) or presence of crizotinib (PF; 200 nmol/L) for 48 hours, after which cell lysates were prepared and subjected to immunoblot analysis with antibodies to phosphorylated (p) or total forms of MET, AKT, ERK, or STAT3, to caspase-3, to PARP, or to β-actin (loading control). The cleaved (cl) forms of caspase-3 and PARP are indicated. C, cells were incubated as in B, after which the number of apoptotic cells was determined by staining with Annexin V followed by flow cytometry. Data are means ± SD from 3 independent experiments. *, $P < 0.05$ versus the corresponding control value.

Pfizer Global Research & Development, and BEZ235 and AZD6244 were from ShangHai Biochempartner.

Immunoblot analysis

Cells were washed twice with ice-cold PBS and then lysed with 1× Cell Lysis Buffer (Cell Signaling Technology) containing 20 mmol/L Tris-HCl (pH 7.5), 150 mmol/L NaCl, 1 mmol/L EDTA (disodium salt), 1 mmol/L EGTA, 1% Triton X-100, 2.5 mmol/L sodium pyrophosphate, 1 mmol/L β-glycerophosphate, 1 mmol/L Na_3VO_4, leupeptin (1 μg/mL), and 1 mmol/L phenylmethylsulfonyl fluoride. The protein concentration of cell lysates was determined with a BCA Protein Assay Kit (Thermo Fisher Scientific), and equal amounts of protein were subjected to SDS-PAGE on a 7.5% or 12% gel (Bio-Rad). The separated proteins were transferred to a nitrocellulose membrane, which was then incubated with Blocking One solution (Nacalai Tesque) for 20 minutes at room temperature before incubation overnight at 4°C with primary antibodies. Rabbit polyclonal antibodies to phosphorylated human MET (pY1234/pY1235), total AKT, phosphorylated AKT, phosphorylated extracellular signal–regulated kinase (ERK), total STAT3, phosphorylated STAT3 (phospho-Tyr705), PARP, caspase-3, BIM, Bcl-2, and X-linked inhibitor of apoptosis protein (XIAP) were obtained from Cell Signaling Technology; those to total ERK were from Santa Cruz Biotechnology; those to total MET were from Zymed/Invitrogen; those to survivin were from Novus; those to c-IAP1 were from R&D Systems; and those to β-actin were from Sigma. All antibodies were used at a 1:1,000 dilution, with the exception of those to β-actin (1:200). The membrane was then washed with PBS containing 0.05% Tween-20 before incubation for 1 hour at room temperature with horseradish peroxidase–conjugated secondary antibodies (GE Healthcare). Immune complexes were finally detected with ECL Western Blotting Detection Reagents (GE Healthcare).

Gene silencing

Cells were plated at 50% to 60% confluence in 6-well plates or 25-cm^2 flasks and then incubated for 24 hours before transient transfection for the indicated times with siRNAs mixed with the Lipofectamine reagent (Invitrogen). The siRNAs specific for MET (MET-1, 5′-ACAAGAUCGUCAACAAAAA-3′; MET-2, 5′-CUACAGAAAUGGUUUCAAA-3′), BIM (BIM-1, 5′-GGAGGGUAUUUUUGAAUAA-3′; BIM-2, 5′-AGGAGGGUAUUUUUGAAUA-3′), or AKT (AKT-1, 5′-CCAGGUAUUUUGAUGAGGA-3′; AKT-2, 5′-CAACCGCCAUCCAGACUGU-3′) mRNAs, as well as corresponding scrambled (control) siRNAs were obtained from Nippon EGT. The data presented for the effects of MET, BIM, or AKT depletion were obtained with the corresponding siRNA-1, but similar results were obtained with each siRNA-2.

Annexin V–binding assay

The binding of Annexin V to cells was measured with the use of an Annexin-V-FLUOS Staining Kit (Roche).

Published OnlineFirst June 22, 2012; DOI: 10.1158/1535-7163.MCT-11-0934

Cells were harvested by exposure to trypsin-EDTA, washed with PBS, and centrifuged at 200 × *g* for 5 minutes. The cell pellets were resuspended in 100 μL of Annexin-V-FLUOS labeling solution, incubated for 10 to 15 minutes at 15° to 25°C, and then analyzed for fluorescence with a flow cytometer (FACSCalibur) and Cell Quest software (Becton Dickinson).

Cell growth inhibition assay

Cells were transferred to 96-well flat-bottomed plates and cultured for 24 hours before exposure to various concentrations of crizotinib for 72 hours. Tetra Color One (5 mmol/L tetrazolium monosodium salt and 0.2 mmol/L 1-methoxy-5-methyl phenazinium methylsulfate; Seikagaku Kogyo) was then added to each well, and the cells were incubated for 3 hours at 37°C before measurement of absorbance at 490 nm with a Multiskan Spectrum instrument (Thermo Labsystems). Absorbance values were expressed as a percentage of that for untreated cells, and the concentration of crizotinib resulting in 50% growth inhibition (IC_{50}) was calculated.

Growth inhibition assay *in vivo*

All animal studies were conducted in accordance with the Recommendations for Handling of Laboratory Animals for Biomedical Research compiled by the Committee on Safety and Ethical Handling Regulations for Laboratory Animal Experiments, Kinki University (Osaka, Japan). The ethical procedures followed conformed to the guidelines of the United Kingdom Co-ordinating Committee on Cancer Research (12). Tumors cells (5×10^6) were injected subcutaneously into the axilla of 5- to 6-week-old female athymic nude mice (BALB/c *nu/nu*; CLEA Japan). Treatment was initiated when tumors in each group of 6 mice achieved an average volume of 300 to 900 mm^3. Treatment groups consisted of vehicle control and crizotinib (25 or 50 mg/kg). Crizotinib was administered by oral gavage daily for 4 weeks, with control animals receiving a 0.5% (w/v) aqueous solution of hydroxypropylmethylcellulose as vehicle. Tumor volume was determined from caliper measurements of tumor length (L) and width (W) according to the formula $LW^2/2$. Both tumor size and body weight were measured twice per week.

Statistical analysis

Quantitative data are presented as means ± SD or SEM from 3 independent experiments or for 6 animals per group, unless indicated otherwise, and were analyzed with the Student 2-tailed t test. A P value of <0.05 was considered statistically significant.

Results

Crizotinib inhibits the proliferation of gastric cancer cells with *MET* amplification

We first examined the effect of the MET-TKI crizotinib on the proliferation of gastric cancer cells positive or negative for *MET* amplification. Six cell lines with *MET* amplification (MKN45, HSC58, 58As1, 58As9, SNU5, Hs746T) were sensitive to crizotinib, with IC_{50} values of less than 200 nmol/L (Table 1). In contrast, crizotinib did not substantially inhibit the proliferation of gastric cancer cells without such gene amplification (Table 1). Transcripts of the *EML4–ALK* fusion gene were not detected in the crizotinib-sensitive gastric cancer cell lines by reverse transcription PCR analysis (data not shown). These data suggested that crizotinib has a marked antiproliferative effect specifically in gastric cancer cells with *MET* amplification.

Table 1. IC_{50} values of crizotinib for inhibition of the growth of gastric cancer cells *in vitro*

Crizotinib response	Cell line	Crizotinib IC_{50}, μmol/L	*MET* amplification
Sensitive	MKN45	0.04	+
	HSC58	0.05	+
	58As1	0.06	+
	58As9	0.17	+
	SNU5	0.03	+
	Hs746T	0.05	+
Resistant	MKN1	8.57	–
	AZ521	1.96	–
	SNU216	4.19	–
	N87	6.10	–
	MKN7	>10	–
	SNU1	0.80	–
	HSC39	2.75	–
	AGS	0.90	–
	MKN28	3.73	–
	NUGC3	2.65	–

NOTE: Data are means of triplicates from experiments that were repeated a total of 3 times with similar results.

Effects of crizotinib on downstream signaling of MET and on apoptosis in gastric cancer cells with or without *MET* amplification

We next examined the effects of crizotinib on phosphorylation of ERK, AKT, and STAT3 in gastric cancer cell lines. Crizotinib markedly inhibited the phosphorylation of ERK, AKT, and STAT3, as well as that of MET in cells with *MET* amplification (Fig. 1B; Supplementary Fig. S1). In contrast, crizotinib had little effect on the phosphorylation of ERK, AKT, or STAT3 in gastric cancer cells without amplification of *MET* (Fig. 1B). Determination of cell-cycle distribution in SNU5, HSC58, 58As1, and 58As9 cells, all of which manifest *MET* amplification, revealed that treatment with crizotinib for 72 hours increased the size of the cell population in sub-G_1 phase, indicative of the induction of apoptosis, as well as reduced that of the cell population in S-phase (Supplementary Fig. S2). We further investigated the effect of crizotinib on apoptosis.

Published OnlineFirst June 22, 2012; DOI: 10.1158/1535-7163.MCT-11-0934

Immunoblot analysis showed that crizotinib triggered the generation of the cleaved forms of caspase-3 and PARP in cells with *MET* amplification but not in those without it (Fig. 1B). Consistent with these results, an Annexin V–binding assay revealed that crizotinib induced a substantial level of apoptosis in *MET* amplification–positive cells but was largely without effect in cell lines without *MET* amplification (Fig. 1C). These data thus suggested that crizotinib inhibits the phosphorylation of ERK, AKT, and STAT3, resulting in induction of apoptosis, in gastric cancer cells with *MET* amplification, whereas such effects were not observed in cells without *MET* amplification.

Effects of crizotinib on the expression of apoptosis-related proteins in *MET* amplification–positive gastric cancer cells

Given that crizotinib induced apoptosis in *MET* amplification–positive gastric cancer cells, we examined the effects of this drug on the expression of apoptosis-related proteins in such cells. Crizotinib upregulated the expression of BIM, a proapoptotic member of the Bcl-2 family of proteins, whereas it had little effect on the expression of other Bcl-2 family members including Bcl-2 (Fig. 2A). Furthermore, crizotinib downregulated the expression of members of the IAP family including survivin, XIAP, and c-IAP1 in cells with *MET* amplification (Fig. 2A).

To verify that the effects of crizotinib on the expression of apoptosis-related proteins in *MET* amplification–positive gastric cancer cells are indeed mediated by MET inhibition rather than by nonspecific inhibition of other kinases, we transfected gastric cancer cells with siRNAs specific for MET mRNA. Transfection with MET siRNAs resulted in a marked decrease in the abundance of MET, which was accompanied by generation of the cleaved forms of both caspase-3 and PARP, in SNU5 and 58As9 cells, both of which manifest *MET* amplification (Fig. 2B). Similar to the effects of crizotinib, depletion of MET by RNA interference (RNAi) also resulted in upregulation of BIM and downregulation of members of the IAP family, whereas it had little effect on the expression of Bcl-2 in such cells (Fig. 2B). These data thus suggested that the upregulation of BIM and the downregulation of members of the IAP family, including survivin, XIAP, and c-IAP1, are related to the induction of apoptosis by the MET inhibitor in gastric cancer cells with *MET* amplification.

Inhibition of the MEK-ERK or PI3K-AKT pathways results in BIM upregulation and survivin downregulation, respectively, in *MET* amplification–positive cells

To identify the signaling pathways responsible for upregulation or downregulation of apoptosis-related proteins by crizotinib, we examined the effects of specific inhibitors of the mitogen-activated protein (MAP)/ERK kinase (MEK) and of phosphoinositide 3-kinase (PI3K) in *MET* amplification–positive cell lines. The MEK inhibitor AZD6244 induced BIM expression without affecting the abundance of the other proteins examined (Fig. 3A), suggesting that expression of BIM is regulated by the MEK-ERK pathway. On the other hand, the PI3K inhibitor BEZ235 reduced the abundance of survivin without affecting that of the other IAP family proteins including c-IAP1 and XIAP (Fig. 3A). We also found that depletion of AKT by RNAi resulted in downregulation of survivin but not of XIAP or c-IAP1 in the *MET* amplification–positive SNU5 and 58As9 cell lines (Fig. 3B). Together, these data suggested that crizotinib regulates BIM and survivin expression through inhibition of the MEK-ERK and PI3K-AKT signaling pathways, respectively, in *MET* amplification–positive gastric cancer cells.

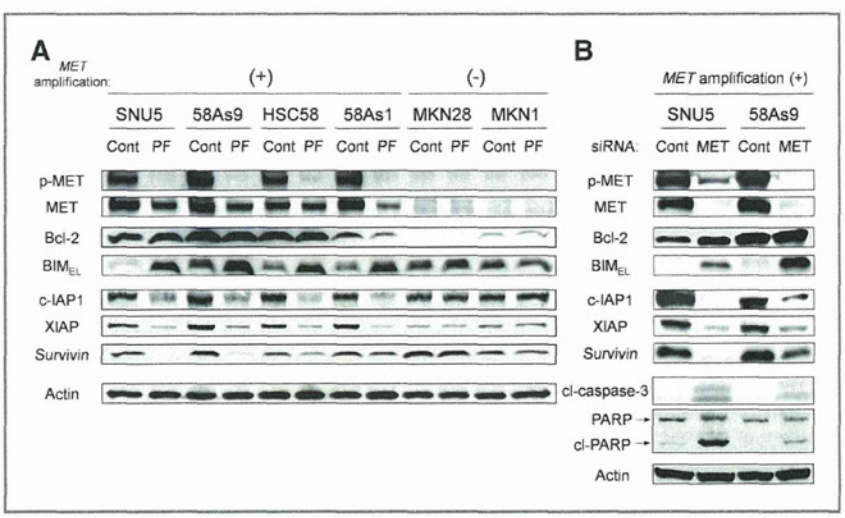

Figure 2. Effects of MET inhibition or depletion on the expression of Bcl-2 family and IAP family proteins in human gastric cancer cells. The indicated cell lines were incubated with or without crizotinib (200 nmol/L) for 24 hours (A) or were transfected with nonspecific (Cont) or MET siRNAs for 48 hours (B), after which cell lysates were prepared and subjected to immunoblot analysis with antibodies to the indicated proteins. The position of the band corresponding to BIM$_{EL}$ is indicated.

Published OnlineFirst June 22, 2012; DOI: 10.1158/1535-7163.MCT-11-0934

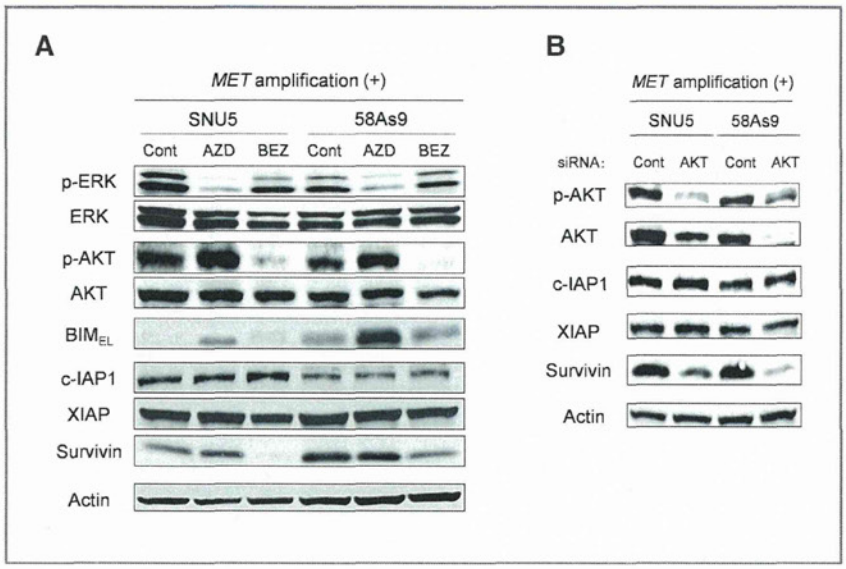

Figure 3. Effects of inhibition of the MEK-ERK or PI3K-AKT signaling pathways on the expression of Bcl-2 family and IAP family proteins in *MET* amplification–positive gastric cancer cells. The indicated cell lines were incubated in the absence (Cont, 0.1% dimethyl sulfoxide) or presence of AZD6244 (0.2 μmol/L) or BEZ235 (0.2 μmol/L) for 24 hours (A) or were transfected with nonspecific (Cont) or AKT siRNAs for 48 hours (B), after which cell lysates were prepared and subjected to immunoblot analysis with antibodies to the indicated proteins.

Role of BIM induction in crizotinib-induced apoptosis in gastric cancer cells with *MET* amplification

Induction of the proapoptotic BH3-only protein BIM has been found to be important for TKI-induced apoptosis in EGF receptor (*EGFR*) gene mutation–positive lung cancer and *HER2* amplification–positive breast cancer (13–17). To investigate whether the upregulation of BIM is related to the induction of apoptosis by crizotinib, we transfected *MET* amplification–positive gastric cancer cells with siRNAs specific for BIM mRNAs. Such transfection resulted in marked inhibition of the upregulation of BIM by crizotinib (Fig. 4A). Immunoblot analysis showed that the attenuation of BIM induction was associated with inhibition of crizotinib-induced apoptosis, as revealed by a reduced extent of caspase-3 and PARP cleavage (Fig. 4A). The Annexin V–binding assay also revealed that such transfection resulted in inhibition of crizotinib-induced apoptosis (Fig. 4B). These data thus suggested that the induction of apoptosis by crizotinib in gastric cancer cells with *MET* amplification is mediated, at least in part, by upregulation of BIM.

Effect of crizotinib on the growth of gastric cancer cells *in vivo*

To determine whether the antitumor action of crizotinib observed *in vitro* might also be apparent *in vivo*, we injected 58As9 cells (positive for *MET* amplification),

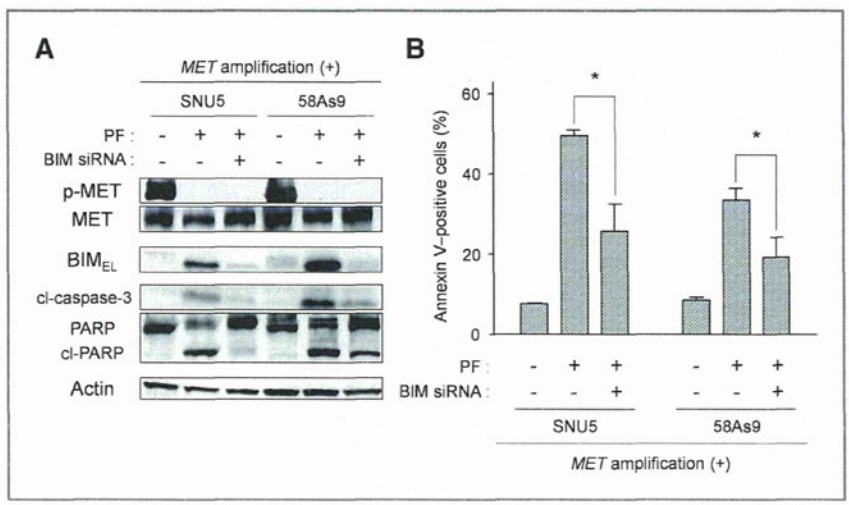

Figure 4. Effect of BIM depletion on apoptosis induced by crizotinib in gastric cancer cells with *MET* amplification. A, the indicated cell lines were transfected with BIM or nonspecific siRNAs for 24 hours and then incubated for 48 hours with or without crizotinib (200 nmol/L). The cells were then lysed and subjected to immunoblot analysis with antibodies to the indicated proteins. B, cells treated as in (A) were assayed for apoptosis by staining with Annexin V followed by flow cytometry. Data are means ± SD from 3 independent experiments. *, $P < 0.05$ for the indicated comparisons.

Published OnlineFirst June 22, 2012; DOI: 10.1158/1535-7163.MCT-11-0934

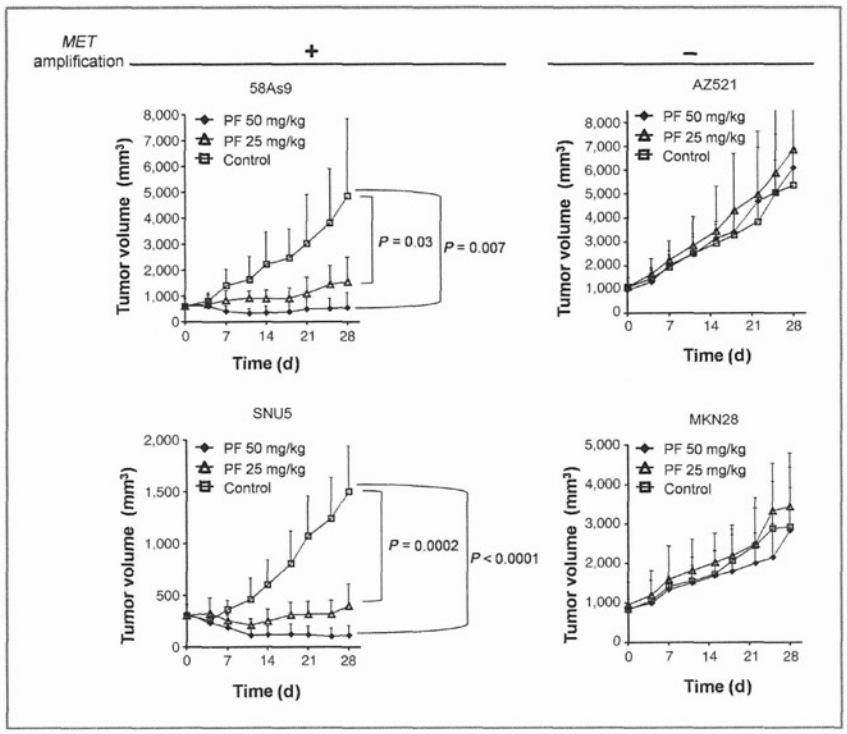

Figure 5. Effect of crizotinib on the growth of gastric cancer cells *in vivo*. Nude mice with tumor xenografts established by subcutaneous injection of 58As9, SNU5, AZ521, or MKN28 cells were treated daily for 4 weeks with vehicle (control) or crizotinib (25 or 50 mg/kg). Tumor volume was determined at the indicated times after the onset of treatment. Data are means ± SEM for 6 mice per group. *P* values are for the indicated comparisons at 28 days.

SNU5 cells (positive for *MET* amplification), AZ521 cells (negative for *MET* amplification), or MKN28 cells (negative for *MET* amplification) into nude mice to elicit the formation of solid tumors. After tumor formation, the mice were treated with vehicle (control) or with crizotinib at a daily dose of 25 or 50 mg/kg by oral gavage for 4 weeks. Crizotinib at either dose eradicated tumors in mice injected with 58As9 or SNU5 cells (Fig. 5; Supplementary Fig. S3). In contrast, tumors in mice injected with AZ521 or MKN28 cells were not affected by crizotinib treatment even at the dose of 50 mg/kg/d (Fig. 5; Supplementary Fig. S3). Treatment with crizotinib at either dose was well-tolerated by the mice, with no signs of toxicity or weight loss during therapy (data not shown). Crizotinib thus exhibited a marked antitumor effect in gastric cancer xenografts positive for *MET* amplification, whereas it had little effect on those negative for *MET* amplification, consistent with our results obtained *in vitro*.

Discussion

Aberrant activation of receptor tyrosine kinase signaling pathways contributes to the development of various types of cancer. Small-molecule inhibitors that target these activated kinases have been developed and have shown substantial efficacy in clinical trials. The identification of patient subgroups that might actually benefit from treatment with such drugs would be expected to optimize their efficacy. The receptor tyrosine kinase MET is considered one such potential target in cancer, and several MET-TKIs are currently undergoing clinical trials in humans. Amplification of *MET* is often responsible for activation of MET signaling, with such amplification occurring frequently in gastric cancer (4–6). We have now shown that crizotinib exerted a marked antitumor action in gastric cancer cells with *MET* amplification. In such gastric cancer cells, attenuation of MET function either by treatment with crizotinib or by MET-targeted RNAi resulted in inhibition of AKT and ERK signaling as well as in the induction of apoptosis, indicating that tumor cells with *MET* amplification are dependent on MET signaling for their growth and survival. Targeting of MET signaling by MET-TKIs is thus a potentially valuable therapeutic strategy for patients with gastric cancer with *MET* amplification.

We also investigated the mediators of crizotinib-induced apoptosis in *MET* amplification–positive gastric cancer cells. We found that crizotinib induced upregulation of BIM, a key proapoptotic member of the Bcl-2 family of proteins that initiates apoptosis signaling by binding to and antagonizing the function of prosurvival Bcl-2 family members (18). Furthermore, depletion of BIM by RNAi resulted in inhibition of crizotinib-induced apoptosis in gastric cancer cells with *MET* amplification, indicating that upregulation of BIM contributes to the induction of apoptosis by the MET-TKI in such cells. These findings are consistent with those of previous studies of lung cancer

Published OnlineFirst June 22, 2012; DOI: 10.1158/1535-7163.MCT-11-0934

cells with *EGFR* mutations and breast cancer cells with *HER2* amplification (13–17). However, our observations revealed that depletion of BIM did not completely abolish crizotinib-induced apoptosis, suggesting that another apoptotic regulator might contribute to MET-TKI–induced apoptotic cell death. We also found that crizotinib induced downregulation of survivin, a member of the IAP family that protects cells against apoptosis by either directly or indirectly inhibiting the activation of effector caspases (19). We found that a PI3K inhibitor or RNAi-mediated depletion of AKT reduced the abundance of survivin, indicating that the expression of survivin is regulated by PI3K-AKT signaling in *MET* amplification–positive gastric cancer cells. Previous studies have shown that the expression of survivin is dependent on PI3K-AKT signaling that operates downstream of receptor tyrosine kinases and is essential for cell survival in *EGFR* mutation–positive non–small cell lung cancer cells as well as in breast cancer cells positive for *HER2* amplification (16, 17). These results suggest that downregulation of survivin via inhibition of the MET-PI3K-AKT pathway likely also contributes to the induction of apoptosis by crizotinib in *MET* amplification–positive gastric cancer cells.

We have shown that crizotinib induced downregulation of XIAP and c-IAP1 in gastric cancer cells with *MET* amplification. We further showed that depletion of MET by RNAi induced downregulation of XIAP and c-IAP1, indicating that these proteins are also regulated by MET signaling in *MET* amplification–positive gastric cancer cells. We investigated which signaling pathway is responsible for downregulation of XIAP and c-IAP1 resulting from inhibition of MET. Given that crizotinib inhibited both ERK and AKT phosphorylation in *MET* amplification–positive cell lines, we examined the effects both of specific inhibitors of MEK and PI3K as well as of siRNAs specific for AKT mRNA in such cells. However, none of these agents induced downregulation of XIAP or c-IAP1 in gastric cancer cells with *MET* amplification. We previously showed that activation of STAT3 is linked to MET signaling and that forced expression of a constitutively active form of STAT3 attenuated MET-TKI–induced apoptosis in MET-activated gastric cancer cells, suggesting that inhibition of STAT3 activity contributes to MET-TKI–induced apoptosis (20). To investigate whether the regulation of XIAP or c-IAP1 expression is mediated by STAT3 signaling, we transfected SNU5 and 58As9 cells, both of which manifest *MET* amplification, with an siRNA that targets STAT3 mRNA. However, depletion of STAT3 by RNAi had no substantial effect on expression of XIAP and c-IAP1 in such cells (data not shown). Previous studies have shown that XIAP and c-IAP1 were not substantially affected by EGFR-TKIs in *EGFR* mutation–positive non–small cell lung cancer cells or by HER2-targeting agents in breast cancer cells positive for *HER2* amplification (16, 17). Given that inhibition of MET results in downregulation of XIAP and c-IAP1 in *MET* amplification–positive gastric cancer cells, the mechanism by which the expression of such proteins is regulated likely differs between MET and other receptor tyrosine kinases including EGFR and HER2. However, the signaling pathway responsible for downregulation of XIAP and c-IAP1 by MET inhibition remains unknown. Further studies are thus required to clarify the regulation of XIAP and c-IAP1 and the contribution of members of the IAP family to MET-TKI–induced apoptosis in gastric cancer cells with *MET* amplification.

In conclusion, our results have shown that crizotinib has pronounced effects on signal transduction and survival in gastric cancer cells with *MET* amplification. Crizotinib has recently been approved for treatment of ALK-driven lung cancer by the FDA on the basis of safety and effectiveness data. The IC_{50} values of crizotinib for inhibition of the growth of *MET* amplification–positive gastric cancer cell lines were lower than the mean trough concentration of the drug achieved in the plasma of patients at steady state (292 ng/mL or 644 nmol/L; ref. 21). Indeed, crizotinib was recently found to exhibit antitumor activity in 2 of 4 patients with *MET* amplification–positive gastroesophageal cancer (22), supporting further study of the molecular mechanism underlying its antitumor action. In the present study, we showed that BIM and IAP family members including survivin, XIAP, and c-IAP1 play a role in crizotinib-induced apoptosis in association with inhibition of MET signaling in gastric cancer cells with *MET* amplification. Our observations provide a basis for the further development of MET-targeted therapy for patients with gastric cancer with *MET* amplification.

Disclosure of Potential Conflicts of Interest

No potential conflicts of interest were disclosed.

Authors' Contributions

Conception and design: W. Okamoto, I. Okamoto, K. Nakagawa
Development of methodology: W. Okamoto, T. Arao, K. Sakai, K. Yanagihara
Acquisition of data (provided animals, acquired and managed patients, provided facilities, etc.): W. Okamoto, I. Okamoto, K. Kuwata, E. Hatashita, H. Yamaguchi, K. Sakai
Analysis and interpretation of data (e.g., statistical analysis, biostatistics, computational analysis): W. Okamoto, I. Okamoto, K. Kuwata, E. Hatashita, H. Yamaguchi
Writing, review, and/or revision of the manuscript: W. Okamoto, I. Okamoto, K. Nishio, K. Nakagawa
Administrative, technical, or material support (i.e., reporting or organizing data, constructing databases): T. Arao, K. Kuwata, E. Hatashita, H. Yamaguchi, K. Sakai, K. Yanagihara
Study supervision: I. Okamoto, K. Nakagawa

Acknowledgments

The authors thank Pfizer for the provision of crizotinib (PF-02341066) used in this study.

Grant Support

The authors received no grant support for this study.

The costs of publication of this article were defrayed in part by the payment of page charges. This article must therefore be hereby marked *advertisement* in accordance with 18 U.S.C. Section 1734 solely to indicate this fact.

Received November 16, 2011; revised March 30, 2012; accepted April 11, 2012; published OnlineFirst June 22, 2012.

Published OnlineFirst June 22, 2012; DOI: 10.1158/1535-7163.MCT-11-0934

References

1. Hartgrink HH, Jansen EP, van Grieken NC, van de Velde CJ. Gastric cancer. Lancet 2009;374:477–90.
2. Wesolowski R, Lee C, Kim R. Is there a role for second-line chemotherapy in advanced gastric cancer? Lancet Oncol 2009;10: 903–12.
3. Bang YJ, Van Cutsem E, Feyereislova A, Chung HC, Shen L, Sawaki A, et al. Trastuzumab in combination with chemotherapy versus chemotherapy alone for treatment of HER2-positive advanced gastric or gastro-oesophageal junction cancer (ToGA): a phase 3, open-label, randomised controlled trial. Lancet 2010;376:687–97.
4. Kuniyasu H, Yasui W, Kitadai Y, Yokozaki H, Ito H, Tahara E. Frequent amplification of the c-met gene in scirrhous type stomach cancer. Biochem Biophys Res Commun 1992;189:227–32.
5. Nessling M, Solinas-Toldo S, Wilgenbus KK, Borchard F, Lichter P. Mapping of chromosomal imbalances in gastric adenocarcinoma revealed amplified protooncogenes MYCN, MET, WNT2, and ERBB2. Genes Chromosomes Cancer 1998;23:307–16.
6. Sakakura C, Mori T, Sakabe T, Ariyama Y, Shinomiya T, Date K, et al. Gains, losses, and amplifications of genomic materials in primary gastric cancers analyzed by comparative genomic hybridization. Genes Chromosomes Cancer 1999;24:299–305.
7. Smolen GA, Sordella R, Muir B, Mohapatra G, Barmettler A, Archibald H, et al. Amplification of MET may identify a subset of cancers with extreme sensitivity to the selective tyrosine kinase inhibitor PHA-665752. Proc Natl Acad Sci U S A 2006;103:2316–21.
8. Okamoto W, Okamoto I, Yoshida T, Okamoto K, Takezawa K, Hatashita E, et al. Identification of c-Src as a potential therapeutic target for gastric cancer and of MET activation as a cause of resistance to c-Src inhibition. Mol Cancer Ther 2010;9:1188–97.
9. Zou HY, Li Q, Lee JH, Arango ME, McDonnell SR, Yamazaki S, et al. An orally available small-molecule inhibitor of c-Met, PF-2341066, exhibits cytoreductive antitumor efficacy through antiproliferative and antiangiogenic mechanisms. Cancer Res 2007;67:4408–17.
10. Tanizaki J, Okamoto I, Okamoto K, Takezawa K, Kuwata K, Yamaguchi H, et al. MET tyrosine kinase inhibitor crizotinib (PF-02341066) shows differential antitumor effects in non-small cell lung cancer according to MET alterations. J Thorac Oncol 2011;6:1624–31.
11. Yanagihara K, Takigahira M, Tanaka H, Komatsu T, Fukumoto H, Koizumi F, et al. Development and biological analysis of peritoneal metastasis mouse models for human scirrhous stomach cancer. Cancer Sci 2005;96:323–32.
12. United Kingdom Co-ordinating Committee on Cancer Research (UKCCCR). Guidelines for the welfare of animals in experimental neoplasia (second edition). Br J Cancer 1998;77:1–10.
13. Costa DB, Halmos B, Kumar A, Schumer ST, Huberman MS, Boggon TJ, et al. BIM mediates EGFR tyrosine kinase inhibitor-induced apoptosis in lung cancers with oncogenic EGFR mutations. PLoS Med 2007;4:1669–79; discussion 1680.
14. Cragg MS, Kuroda J, Puthalakath H, Huang DC, Strasser A. Gefitinib-induced killing of NSCLC cell lines expressing mutant EGFR requires BIM and can be enhanced by BH3 mimetics. PLoS Med 2007;4:1681–89; discussion 1690.
15. Gong Y, Somwar R, Politi K, Balak M, Chmielecki J, Jiang X, et al. Induction of BIM is essential for apoptosis triggered by EGFR kinase inhibitors in mutant EGFR-dependent lung adenocarcinomas. PLoS Med 2007;4:e294.
16. Okamoto K, Okamoto I, Okamoto W, Tanaka K, Takezawa K, Kuwata K, et al. Role of survivin in EGFR inhibitor-induced apoptosis in non-small cell lung cancers positive for EGFR mutations. Cancer Res 2010;70:10402–10.
17. Tanizaki J, Okamoto I, Fumita S, Okamoto W, Nishio K, Nakagawa K. Roles of BIM induction and survivin downregulation in lapatinib-induced apoptosis in breast cancer cells with HER2 amplification. Oncogene 2011;30:4097–106.
18. Chen L, Willis SN, Wei A, Smith BJ, Fletcher JI, Hinds MG, et al. Differential targeting of prosurvival Bcl-2 proteins by their BH3-only ligands allows complementary apoptotic function. Mol Cell 2005;17: 393–403.
19. Hengartner MO. The biochemistry of apoptosis. Nature 2000;407: 770–6.
20. Okamoto W, Okamoto I, Arao T, Yanagihara K, Nishio K, Nakagawa K. Differential roles of STAT3 depending on the mechanism of STAT3 activation in gastric cancer cells. Br J Cancer 2011;105: 407–12.
21. Bang YJ, Kwak EL, Shaw AT, Camidge DR, Iafrate AJ, Maki RG, et al. Clinical activity of the oral ALK inhibitor PF-02341066 in ALK-positive patients with non-small cell lung cancer (NSCLC). J Clin Oncol 28:18s, 2010 (suppl; abstr 3).
22. Lennerz JK, Kwak EL, Ackerman A, Michael M, Fox SB, Bergethon K, et al. MET amplification identifies a small and aggressive subgroup of esophagogastric adenocarcinoma with evidence of responsiveness to crizotinib. J Clin Oncol 2011;29:4803–10.

Annals of Oncology 23: 2931–2936, 2012
doi:10.1093/annonc/mds124
Published online 5 July 2012

Clinical outcome for *EML4-ALK*-positive patients with advanced non-small-cell lung cancer treated with first-line platinum-based chemotherapy

M. Takeda[1], I. Okamoto[1]*, K. Sakai[2], H. Kawakami[1], K. Nishio[2] & K. Nakagawa[1]

[1]*Departments of Medical Oncology;* [2]*Genome Biology, Kinki University Faculty of Medicine, Osaka-Sayama, Japan*

Received 16 February 2012; revised 19 March 2012; accepted 20 March 2012

Background: The *EML4-ALK* fusion oncogene represents a recently identified molecular target in a subset of patients with non-small-cell lung cancer (NSCLC). Limited data have been available, however, on the outcome of first-line platinum-based chemotherapy in patients with *EML4-ALK*-positive advanced NSCLC who have not been treated with an ALK kinase inhibitor.

Patients and methods: The efficacy of platinum-based chemotherapy was compared between patients with advanced nonsquamous NSCLC who harbor *EML4-ALK* and those who harbor *EGFR* mutations and those with neither molecular abnormality.

Results: Among 200 patients with advanced nonsquamous NSCLC, 18 (9.0%) were positive for *EML4-ALK*, 31 (15.5%) harbored *EGFR* mutations, and 151 (75.5%) were wild type for both abnormalities. Platinum-based combination chemotherapy showed similar efficacies in the *EML4-ALK*, *EGFR* mutation, and wild-type cohorts in terms of response rate and progression-free survival, and overall survival in the *EML4-ALK* cohort closely resembled that in the wild-type cohort. Within the *EML4-ALK* cohort, patients with variants 1 or 3 of the fusion gene were predominant and did not appear to differ in their sensitivity to the platinum-based regimens.

Conclusion: Patients with *EML4-ALK*-positive advanced NSCLC manifest an aggressive clinical course similar to that of those with wild-type tumors if the effective targeted therapy is not instituted.

Key words: anaplastic lymphoma kinase, epidermal growth factor receptor, non-small-cell lung cancer, platinum-based chemotherapy

introduction

Recent insight into the molecular basis of lung cancer has led to changes in the treatment of this disease. The identification of somatic mutations in the epidermal growth factor receptor (*EGFR*) gene in a subset of patients with non-small-cell lung cancer (NSCLC) has thus led to the treatment of such patients with EGFR tyrosine kinase inhibitors (TKIs) and a consequent superior response rate, prolonged progression-free survival (PFS), and improved quality of life compared with those achieved with cytotoxic chemotherapy [1, 2]. Fusion of the anaplastic lymphoma kinase (*ALK*) gene and the echinoderm microtubule-associated protein-like 4 gene (*EML4*) in NSCLC was also identified in 2007 [3]. The *EML4-ALK* fusion gene is generated by an inv(2)(p21p23) chromosomal translocation, and it shows oncogenic activity in a mouse model [4]. Several *EML4-ALK* fusion variants have been identified to date, with the most frequent being variants 1 and 3 [3, 5–8], and between 3% and 13% of lung tumors have been found to harbor *EML4-ALK* fusions [3, 9, 10]. Preclinical and clinical studies have shown that cancer cells harboring *EML4-ALK* or other *ALK* abnormalities are highly sensitive to ALK inhibition. In a recent phase I clinical trial, crizotinib (PF-02341066), an inhibitor of the tyrosine kinase activity of both ALK and the proto-oncoprotein MET, showed marked antitumor activity in NSCLC patients with *ALK* abnormalities, with an objective response rate of 61% and median PFS of 10 months [11].

Limited data have been available, however, regarding overall survival (OS) of patients with *EML4-ALK*-positive advanced NSCLC who have not been treated with ALK kinase inhibitors. Although several studies have evaluated the efficacy of cytotoxic chemotherapy based on the molecular profile of the disease, classified as *EML4-ALK* positive, *EGFR* mutation positive, or wild type for both types of genetic abnormality [10, 12–15], it has remained unclear whether *EML4-ALK* is an effective prognostic factor [13–15]. Further studies are thus warranted to determine the impact of *EML4-ALK* on the survival of patients treated with cytotoxic chemotherapy.

*Correspondence to: Dr I. Okamoto, Department of Medical Oncology, Kinki University Faculty of Medicine, 377-2 Ohno-higashi, Osaka-Sayama, Osaka 589-8511, Japan. Tel: +81-72-366-0221; Fax: +81-72-360-5000; E-mail: chi-okamoto@dotd.med.kindai.ac.jp

In the present study, a large series of patients with advanced nonsquamous NSCLC not previously treated with an ALK inhibitor was screened for *EML4-ALK* by analysis of formalin-fixed paraffin-embedded (FFPE) tissue specimens obtained by lung biopsy. We evaluated the efficacy of platinum-based chemotherapy according to the molecular profile of the tumors, which were classified as positive for *EML4-ALK*, positive for *EGFR* mutation, or wild type for both types of genetic abnormality. In addition, we undertook an exploratory analysis of the efficacy of platinum-based chemotherapy according to the specific variant of *EML4-ALK* detected.

patients and methods

patients

The present study recruited consecutive patients with advanced nonsquamous NSCLC who were treated with first-line platinum-based combination chemotherapy at Kinki University Hospital between February 2003 and October 2011. Patients met all the following criteria: a histological diagnosis of nonsquamous NSCLC with at least one measurable lesion; a clinical stage of IIIB or IV; an Eastern Cooperative Oncology Group performance status of 0 or 1; and availability of both complete clinical information and FFPE tissue blocks suitable for genetic analysis of *EML4-ALK* and *EGFR*. The choice of first-line chemotherapy regimen was made by the treating physician. Patients who received an EGFR-TKI as first-line treatment or those who received an ALK inhibitor such as crizotinib in any line were excluded from the study. Tumor response was examined by computed tomography and was evaluated according to the RECIST version 1.1. The study protocol was approved by the local institutional review board with the conditions that tissue samples be processed anonymously and analyzed only for somatic mutations (not for germ line mutations) and that the study be disclosed publicly, according to the Ethical Guidelines for Human Genome Research published by the Ministry of Education, Culture, Sports, Science, and Technology, the Ministry of Health, Labor, and Welfare, and the Ministry of Economy, Trade, and Industry of Japan. The present study also conforms to the provisions of the Declaration of Helsinki.

detection of *EML4-ALK* variants and nucleotide sequencing

Total RNA was extracted from FFPE tissue with the use of an RNeasy FFPE Kit (Qiagen, Valencia, CA) and was subjected to reverse transcription with the use of a High Capacity complementary DNA (cDNA) Reverse Transcription Kit (Applied Biosystems, Foster City, CA). The resulting cDNAs for *EML4-ALK* fusions (variants 1, 2, 3a, 3b, 4, 5a, 5b, 6, and 7) were detected with the MassARRAY iPLEX platform (Sequenom, San Diego, CA), which involves a three-step process consisting of the PCR, single-base primer extension, and separation of the products on a matrix-loaded silicon chip by MALDI–TOF (matrix-assisted laser desorption-ionization–time of flight) mass spectrometry [16]. Data analysis was performed with MassARRAY Typer software version 4.0 (Sequenom). PCR products were subcloned into the TOPO TA pCR2.1 vector (Invitrogen, San Diego, CA) and sequenced with an automated sequencer (ABI Prism 3100 Genetic Analyzer; Applied Biosystems) with the use of M13 universal primers. *EGFR* mutations that confer sensitivity to EGFR-TKIs were identified either by the Scorpion amplified refractory mutation system or by the PCR-Invader method (BML, Tokyo, Japan).

statistical analysis

Analyzed variables include age, sex, smoking history, tumor histology, clinical stage, and molecular abnormality. Differences in demographic characteristics and treatment response between two subgroups were evaluated with the two-sided Fisher's exact test; Student's *t*-test was performed to compare continuous variables between two subgroups. PFS was calculated from the date of chemotherapy initiation either to the date of progression or death without demonstrated disease progression or to the date of last contact. OS was calculated from the date of chemotherapy initiation to the date of death from any cause or to the date of last contact. The probability of survival as a function of time was estimated with the Kaplan–Meier method, and the difference in survival between subgroups of patients was evaluated with the log-rank test. The hazard ratio (HR) for two subgroups of patients was estimated by proportional hazards regression with a 95% confidence interval (CI). A P value of < 0.05 was considered statistically significant. All statistical analysis was performed with GraphPad Prism software (version 5.0; GraphPad Software, San Diego, CA).

results

patient characteristics

We analyzed tumor specimens from 200 of 290 consecutive patients with advanced nonsquamous NSCLC who were treated with first-line platinum-based chemotherapy during the study period. The remaining 90 patients were excluded because there was no or insufficient tumor tissue available for genetic analysis. The baseline characteristics of the 200 enrolled patients are summarized in Table 1. They included 127 (64%) men, 84 (42%) never or light smokers, 178 (89%) individuals with adenocarcinoma, and 163 (82%) patients with disease of stage IV, with the median age of the entire group being 63 years (range, 29–81). The patients were divided into three groups on the basis of the molecular subtype of NSCLC: *EML4-ALK* positive ($n = 18$), *EGFR* mutation positive ($n = 31$), and wild type ($n = 151$). Among the 31 patients with *EGFR* mutations, 15 individuals (48%) had a deletion in exon 19 and 14 individuals (45%) had a point mutation (L858R or L861Q) in exon 21; 18 patients (58%) were treated during the first half of the study period (from 2003 to 2007) and 13 patients (42%) during the second half (from 2007 to 2011). Patients in the wild-type subgroup harbored neither *EGFR* mutations nor *EML4-ALK*. One patient harboring both *EML4-ALK* and an *EGFR* mutation was classified as *EML4-ALK* positive. The 18 (9.0%) patients positive for *EML4-ALK* were significantly younger (median age, 46 years) than were the *EGFR* mutation-positive patients (median age, 63 years; $P < 0.001$) or the wild-type patients (median age, 64 years; $P < 0.001$). There were no significant differences among the three subgroups with respect to sex, smoking history, tumor histology, or disease stage.

efficacy of platinum-based combination chemotherapy according to molecular subtype of NSCLC

We evaluated the efficacy of platinum-based chemotherapy according to the molecular profile of NSCLC. Several chemotherapy regimens were implemented in the study population (supplemental Table S1, available at *Annals of*

Table 1. Patient characteristics according to genetic status of NSCLC

Variable	Total ($n = 200$)	*EML4-ALK*$^+$ ($n = 18$)	*EML4-ALK*$^-$ ($n = 182$)		*P*	
			EGFR mutation$^+$ ($n = 31$)	*EGFR* mutation$^-$ ($n = 151$)	*EML4-ALK*$^+$ versus *EGFR* mutation$^+$	*EML4-ALK*$^+$ versus wild type
Age (years)						
Median	63	46	63	64	<0.001	<0.001
Range	29–81	29–69	44–75	35–81		
Sex						
Male	127 (64%)	9 (50%)	12 (39%)	106 (70%)	0.553	0.108
Female	73 (37%)	9 (50%)	19 (61%)	45 (30%)		
Smoking status[a]						
Never	65 (33%)	6 (33%)	16 (52%)	43 (28%)	0.559*	0.125*
Light smoker	19 (10%)	4 (22%)	4 (13%)	11 (7%)		
Smoker	116 (58%)	8 (44%)	11 (35%)	97 (64%)		
Histology						
Adenocarcinoma	178 (89%)	16 (89%)	30 (97%)	132 (87%)	0.546**	1.000**
Large cell	6 (3%)	1 (6%)	1 (3%)	4 (3%)		
Adenosquamous	2 (1%)	1 (6%)	0	1 (1%)		
NOS	14 (7%)	0	0	14 (9%)		
Stage						
IIIB	37 (19%)	4 (22%)	5 (16%)	28 (19%)	0.708	0.751
IV	163 (82%)	14 (78%)	26 (84%)	123 (81%)		

[a]Light smokers, ≤10 pack years; smokers, >10 pack years.

*P value calculated by binary comparison (never or light smokers versus smokers). **P value calculated by binary comparison (adenocarcinoma versus nonadenocarcinoma). NSCLC, non-small-cell lung cancer; NOS, not otherwise specified.

Table 2. Efficacy of first-line platinum-based treatment based on genetic status of NSCLC

Response	*EML4-ALK*$^+$ ($n = 18$)	*EML4-ALK*$^-$ ($n = 182$)		*P*	
		EGFR mutation$^+$ ($n = 31$)	*EGFR* mutation$^-$ ($n = 151$)	*EML4-ALK*$^+$ versus *EGFR* mutation$^+$	*EML4-ALK*$^+$ versus wild type
CR	1 (6%)	0	1 (1%)		
PR	7 (39%)	14 (45%)	58 (38%)		
SD	6 (33%)	13 (42%)	52 (34%)		
PD	4 (22%)	4 (13%)	40 (26%)		
ORR	8 (44%)	14 (45%)	59 (39%)	1.000	0.800

NSCLC, non-small-cell lung cancer; CR, complete response; PR, partial response; SD, stable disease; PD, progressive disease; ORR, overall response rate.

Oncology online). The *EML4-ALK*-positive cohort included 7 (39%) individuals treated with platinum plus pemetrexed, compared with 4 (13%, $P = 0.072$) and 25 (17%, $P = 0.049$) such individuals in the *EGFR* mutation-positive and wild-type cohorts, respectively. Among the entire study population, 20 (10%) individuals received bevacizumab together with platinum-based doublet chemotherapy [2 (11%), 1 (3%), and 17 (11%) patients in the *EML4-ALK*, *EGFR*-mutation, and wild-type subgroups, respectively]. Cisplatin was administered in 7 (39%), 12 (39%), and 26 (17%) patients in the *EML4-ALK*, *EGFR*-mutation, and wild-type cohorts, respectively.

All patients were assessable for treatment outcome (Table 2). No significant difference in overall response rate was apparent among the three arms (44%, 45%, and 39% for the *EML4-ALK*, *EGFR*-mutation, and wild-type subgroups, respectively). PFS also did not differ significantly between patients with *EML4-ALK* [median, 6.5 months (95% CI 2.4–10.6)] and either those with *EGFR* mutations [median, 6.0 months (95% CI 5.2–6.8); HR, 0.78 (95% CI 0.42–1.48); $P = 0.452$] or those with neither type of molecular abnormality [median, 4.3 months (95% CI 3.4–5.2); HR, 0.82 (95% CI 0.49–1.36); $P = 0.437$] (Figure 1A).

survival outcome of *EML4-ALK*-positive patients

After a median follow-up of 10.8 months (range, 0.6–75.3) from the start of platinum-based treatment, 91 patients were still alive at last contact. Kaplan–Meier curves for OS of the three cohorts are shown in Figure 1B. *EML4-ALK*-positive patients had an OS similar to that of wild-type patients [median OS, 15.7 months (95% CI 6.2–25.3) versus 15.2

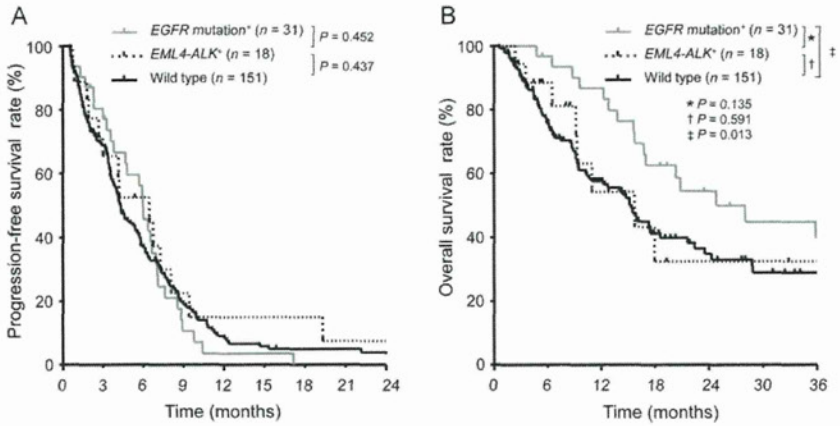

Figure 1. Progression-free survival (A) and overall survival (B) for platinum-based cytotoxic chemotherapy according to genetic status of NSCLC.

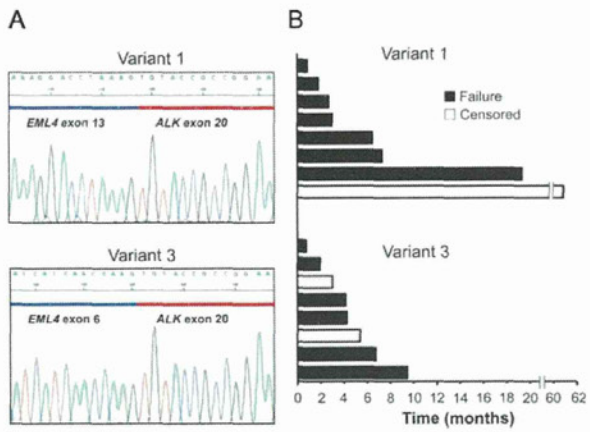

Figure 2. Progression-free survival according to *EML4-ALK* variant. (A) Representative sequence electrophoretograms for tissue specimens harboring *EML4-ALK* variant 1 or variant 3a. (B) Waterfall plot of PFS for the eight patients found to harbor variant 1 and the eight patients found to harbor variant 3 of *EML4-ALK*. Patients still on treatment but censored for progression at the time of analysis are shown as white bars; those who experienced a treatment failure event during the observation period of the study are shown as black bars.

months (95% CI 11.6–18.7), respectively; HR, 0.83 (95% CI 0.42–1.63); $P = 0.591$]. The OS of *EGFR* mutation-positive patients [median, 24.8 months (95% CI 14.1–35.5)] tended to be longer than that of the *EML4-ALK*-positive cohort, but this difference was not statistically significant [HR, 0.47 (95% CI 0.17–1.27); $P = 0.135$]. The OS of *EGFR* mutation-positive patients was significantly greater than that of wild-type patients [HR, 0.56 (95% CI 0.36–0.89); $P = 0.013$].

comparison of PFS between patients with different *EML4-ALK* variants

The genomic breakpoint in the 18 patients with *EML4-ALK* was verified by cloning and sequencing. Eight of these tumors (44%) were found to harbor *EML4-ALK* variant 1, two (11%) had variant 2, and eight (44%) had variant 3 (Figure 2A). To compare the efficacy of platinum-based chemotherapy between patients with different *EML4-ALK* variants, we determined PFS for those with variant 1 and those with variant 3 (Figure 2B). Waterfall plot analysis showed that the median PFS was similar in both groups (4.8 and 4.3 months for variants 1 and 3, respectively). However, platinum-based combination chemotherapy showed long-term efficacy in two patients with variant 1; one patient received four cycles of chemotherapy with pemetrexed and carboplatin followed by maintenance pemetrexed therapy for 19.3 months until disease progression, whereas the other patient received six cycles of chemotherapy with carboplatin and S-1 and showed no evidence of disease progression for 60.9 months.

discussion

Our present study population comprised 200 patients with advanced nonsquamous NSCLC who were treated with first-line platinum-based chemotherapy and for whom sufficient tissue was available in paraffin blocks for genetic analysis of

EML4-ALK and *EGFR*. For detection of *EML4-ALK* transcripts, we applied reverse transcription and the MassARRAY system, which is based on PCR and MALDI–TOF mass spectrometry and which shows a high degree of concordance with fluorescence *in situ* hybridization [16]. The frequency of *EML4-ALK* in our present study (9.0%) is consistent with that reported in previous studies [3, 9, 10]. The frequency of *EGFR* mutations in our study (15.5%) is lower than that previously determined for Asian patients with nonsquamous NSCLC [17]; the reason for this difference is that *EGFR* mutation-positive patients who received first-line treatment with EGFR-TKIs were excluded from our analysis, with EGFR-TKIs now being a treatment option for chemotherapy-naive *EGFR* mutation-positive patients on the basis of recent phase III trials comparing EGFR-TKIs with platinum-based chemotherapy [1, 2]. We observed that the demographics of *EML4-ALK*-positive patients differed from those of fusion-negative patients. Consistent with previous studies, we found that *EML4-ALK*-positive patients were significantly younger than *EGFR* mutation-positive or wild-type patients [10, 12, 18, 19]. The proportion of never and light smokers was found not to differ significantly according to *EML4-ALK* status, although the proportion tended to be higher in *EML4-ALK*-positive patients than in wild-type patients ($P = 0.125$).

Crizotinib, the first clinically available TKI that targets ALK, has shown pronounced single-agent activity in patients with *EML4-ALK*-positive NSCLC [11]. The sensitivity of such patients to platinum-based combination chemotherapy relative to that of patients whose tumors are negative for *EML4-ALK* has remained unclear, however. Two retrospective studies have investigated whether the tumor molecular profile affects sensitivity to platinum-based combination chemotherapy in advanced NSCLC [10, 12]. These studies did not detect a significant difference in response rate or PFS among patients who were *EML4-ALK* positive, *EGFR* mutation positive, or wild type, although the cytotoxic drug partnered with the platinum agent was not specified. Consistent with these findings, we have now shown that patients in the *EML4-ALK*, *EGFR*-mutation, and wild-type cohorts exhibited similar sensitivity to platinum-based combination chemotherapy in terms of response rate and PFS. These results suggest that sensitivity to platinum-based chemotherapy is not influenced by *EML4-ALK* status in patients with advanced NSCLC.

Limited data are available regarding OS of patients with *EML4-ALK*-positive advanced NSCLC who have not been treated with an ALK kinase inhibitor. Altavilla et al. [14] found that, among 40 patients treated with cisplatin and pemetrexed as first-line combination chemotherapy, the median OS was 17 months for *EML4-ALK*-positive patients ($n = 8$) compared with 11 months for *EML4-ALK*-negative patients ($n = 32$). Wu et al. [15] showed that, among patients wild type for *EGFR* who received either monotherapy or platinum-doublet chemotherapy, those positive for *EML4-ALK* had a superior OS (14.7 months) compared with those negative for the fusion gene (10.3 months). In contrast to these findings, a recent study showed that the OS of crizotinib-naive, *EML4-ALK*-positive patients with advanced NSCLC did not differ significantly from that of wild-type patients, although details regarding the first-line chemotherapy, given either as a platinum-based doublet or as a single agent, are unclear [13]. These apparent discrepancies may be explained by an unbalanced distribution of platinum-doublet chemotherapy between *EML4-ALK*-positive and -negative subgroups. Given that platinum-based chemotherapy yields a substantial survival advantage in patients with advanced NSCLC [20], we assessed OS according to the tumor molecular profile in selected NSCLC patients who were offered treatment with platinum-based combination chemotherapy. Furthermore, given that *EML4-ALK*-positive patients who received an ALK inhibitor such as crizotinib in any line were excluded from our study, the *EML4-ALK*-positive cohort represents the natural history of advanced NSCLC positive for the fusion gene in the absence of effective targeted therapy. We found that OS in the *EML4-ALK* cohort closely resembled that in the wild-type cohort (15.7 versus 15.2 months, respectively). Favorable outcomes achieved in the wild-type cohort are likely related to the fact that 104 of 151 patients (69%) received subsequent treatment, including 19 (13%) patients treated with an EGFR-TKI. In the *EGFR* mutation-positive cohort, most (84%) patients received an EGFR-TKI as second-line or later chemotherapy. EGFR-TKIs have been found to yield a substantial clinical benefit in terms of OS, even when the drug is administered as second-line or later chemotherapy [21, 22]. A trend toward an OS advantage in the *EGFR* mutation-positive cohort (24.8 months) compared with the *EML4-ALK* and wild-type cohorts is likely attributable to the difference in the availability of EGFR-TKI treatment among the three groups. These results indicate that, in the absence of treatment with ALK inhibitors, *EML4-ALK* status does not have prognostic value in patients with advanced nonsquamous NSCLC.

Although various break and fusion points within the *EML4* locus give rise to different isoforms of *EML4-ALK*, it is unclear whether there are any differences in the therapeutic response of patients harboring the different variants that might warrant more specific knowledge of *EML4-ALK* status [3, 5–9]. We applied the MassARRAY system for screening of *EML4-ALK*; this system is able to distinguish between the different *EML4-ALK* variants with the use of only a small amount of FFPE tissue. The two most common variants (variants 1 and 3a/b) were identified in 89% of *EML4-ALK*-positive tumors in the present study. Although our exploratory analysis of PFS suggested that treatment efficacy was similar in patients harboring variant 1 and those with variant 3, two patients with variant 1 showed a long-term response to platinum-based combination chemotherapy. These observations warrant confirmation in a prospective study as well as exploration of any biological differences between variants 1 and 3.

In conclusion, our results suggest that *EML4-ALK* status does not affect the sensitivity of patients with advanced NSCLC to platinum-based combination chemotherapy. A randomized phase III study comparing crizotinib with platinum-doublet chemotherapy as the first-line treatment for NSCLC patients harboring *EML4-ALK* is ongoing; patients assigned to platinum-based chemotherapy can crossover to crizotinib treatment when progressive disease is documented. It will therefore be difficult to obtain OS data for crizotinib-

naive patients with *EML4-ALK* who are treated with first-line platinum-based chemotherapy in a prospective cohort study. Our present study has shown that *EML4-ALK*-positive patients with advanced NSCLC manifest an aggressive clinical course similar to that of patients with wild-type tumors if the effective targeted therapy is not instituted. Our findings thus underline the importance of the development of ALK inhibitors for this molecularly defined population of NSCLC patients.

funding

This study was not supported by a sponsor or funding agency.

disclosure

The authors have declared no conflicts of interest.

references

1. Mitsudomi T, Morita S, Yatabe Y et al. Gefitinib versus cisplatin plus docetaxel in patients with non-small-cell lung cancer harbouring mutations of the epidermal growth factor receptor (WJTOG3405): an open label, randomised phase 3 trial. Lancet Oncol 2010; 11: 121–128.
2. Maemondo M, Inoue A, Kobayashi K et al. Gefitinib or chemotherapy for non-small-cell lung cancer with mutated EGFR. N Engl J Med 2010; 362: 2380–2388.
3. Soda M, Choi YL, Enomoto M et al. Identification of the transforming EML4-ALK fusion gene in non-small-cell lung cancer. Nature 2007; 448: 561–566.
4. Soda M, Takada S, Takeuchi K et al. A mouse model for EML4-ALK-positive lung cancer. Proc Natl Acad Sci USA 2008; 105: 19893–19897.
5. Takeuchi K, Choi YL, Soda M et al. Multiplex reverse transcription-PCR screening for EML4-ALK fusion transcripts. Clin Cancer Res 2008; 14: 6618–6624.
6. Koivunen JP, Mermel C, Zejnullahu K et al. EML4-ALK fusion gene and efficacy of an ALK kinase inhibitor in lung cancer. Clin Cancer Res 2008; 14: 4275–4283.
7. Martelli MP, Sozzi G, Hernandez L et al. EML4-ALK rearrangement in non-small cell lung cancer and non-tumor lung tissues. Am J Pathol 2009; 174: 661–670.
8. Wong DW, Leung EL, So KK et al. The EML4-ALK fusion gene is involved in various histologic types of lung cancers from nonsmokers with wild-type EGFR and KRAS. Cancer 2009; 115: 1723–1733.
9. Inamura K, Takeuchi K, Togashi Y et al. EML4-ALK fusion is linked to histological characteristics in a subset of lung cancers. J Thorac Oncol 2008; 3: 13–17.
10. Shaw AT, Yeap BY, Mino-Kenudson M et al. Clinical features and outcome of patients with non-small-cell lung cancer who harbor EML4-ALK. J Clin Oncol 2009; 27: 4247–4253.
11. Kwak EL, Bang YJ, Camidge DR et al. Anaplastic lymphoma kinase inhibition in non-small-cell lung cancer. N Engl J Med 2010; 363: 1693–1703.
12. Koh Y, Kim DW, Kim TM et al. Clinicopathologic characteristics and outcomes of patients with anaplastic lymphoma kinase-positive advanced pulmonary adenocarcinoma: suggestion for an effective screening strategy for these tumors. J Thorac Oncol 2011; 6: 905–912.
13. Shaw AT, Yeap BY, Solomon BJ et al. Effect of crizotinib on overall survival in patients with advanced non-small-cell lung cancer harbouring ALK gene rearrangement: a retrospective analysis. Lancet Oncol 2011; 12: 1004–1012.
14. Altavilla G, Santarpia M, Arrigo C et al. EML4-ALK fusion gene in lung adenocarcinoma: a retrospective analysis of the outcome of cisplatin plus pemetrexed treated patients. J Clin Oncol 2010; 28(Suppl): 15s. (Abstr 7610)
15. Wu SG, Kuo YW, Chang YL et al. EML4-ALK translocation predicts better outcome in lung adenocarcinoma patients with wild-type EGFR. J Thorac Oncol 2012; 7: 98–104.
16. Sakai K, Okamoto I, Takezawa K et al. A novel mass spectrometry–based assay for diagnosis of EML4-ALK–positive non–small cell lung cancer. J Thorac Oncol 2012; in press
17. Shigematsu H, Lin L, Takahashi T et al. Clinical and biological features associated with epidermal growth factor receptor gene mutations in lung cancers. J Natl Cancer Inst 2005; 97: 339–346.
18. Camidge DR, Kono SA, Lu X et al. Anaplastic lymphoma kinase gene rearrangements in non-small cell lung cancer are associated with prolonged progression-free survival on pemetrexed. J Thorac Oncol 2011; 6: 774–780.
19. Lee JO, Kim TM, Lee SH et al. Anaplastic lymphoma kinase translocation: a predictive biomarker of pemetrexed in patients with non-small cell lung cancer. J Thorac Oncol 2011; 6: 1474–1480.
20. Azzoli CG, Baker S, Jr, Temin S et al. American Society of Clinical Oncology Clinical Practice Guideline update on chemotherapy for stage IV non-small-cell lung cancer. J Clin Oncol 2009; 27: 6251–6266.
21. Morita S, Okamoto I, Kobayashi K et al. Combined survival analysis of prospective clinical trials of gefitinib for non-small cell lung cancer with EGFR mutations. Clin Cancer Res 2009; 15: 4493–4498.
22. Rosell R, Moran T, Queralt C et al. Screening for epidermal growth factor receptor mutations in lung cancer. N Engl J Med 2009; 361: 958–967.